Vortex ring instability and its sound

By R. Verzicco[1] AND K. Shariff[2]

This work carries earlier finite-difference calculations of the Widnall instability of vortex rings into the late non-linear stage. Plots of energy in azimuthal Fourier modes indicate that low-order modes dominate at large times; their structure and dynamics remain unexplored, however. An attempt was made to calculate the acoustic signal using the theory of Möhring (1978), valid for unbounded flow. This theory shows that only low-order azimuthal modes contribute to the sound. As a check on the effects of axial periodicity and a slip wall at large radius imposed by the numerical scheme, the acoustic integrals were also computed in a truncated region. Half of the terms contributing to the sound have large differences between the two regions, and the results are therefore unreliable. The error is less severe for a contribution involving only the $m = 2$ mode, and its low frequency is consistent with a free elliptic bending wave on a thin ring.

1. Introduction

Many shear flows of practical interest contain large-scale coherent motions, and some aspects of their dynamics must be responsible for the generation of sound (smaller scale motions affect the dynamics of the large scales but themselves radiate as higher order poles). What these aspects might be is difficult to identify from experiments since the most energetic or most visually apparent motions may not be the most radiative and a detailed knowledge of time-dependence is required. It is a usual procedure in fluid dynamics to extract from a flow the most representative structure with the hope that its evolution alone still retains the important features of the whole flow. In the present case the evolution of azimuthal instabilities on an isolated vortex ring is numerically simulated into the late non-linear stage. We are motivated by the following: (i) Observations using phased arrays of microphones which indicate that the acoustic source location in jets is near the end of the potential core where vortex ring structures break down (Bridges & Hussain 1987, p. 309). Implicit in the consideration of a single ring is the premise that the actual breakdown process does not involve interactions between rings. Factors which may be important in reality are enhanced growth-rate and mode selection due to mutual straining and tearing or pairing. (ii) A good fit (Shariff & Leonard 1992, p. 275) of the acoustic frequency of a turbulent vortex ring measured by Zaitsev *et al.* (1990) to the axisymmetric elliptic core ring but a poor fit to the elliptic bending mode. Further studies along these lines were carried out in Zaitsev & Ko'pev (1993)

1 Università di Roma, "La Sapienza", Dipartimento di Meccanica e Aeronautica
2 NASA Ames Research Center

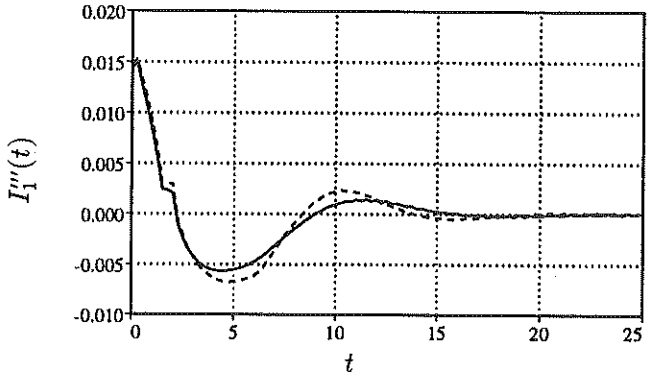

FIGURE 1. Acoustic signal due to axisymmetric elliptically distorted vortex ring. ——— , $\Gamma/\nu = 1200$; ---- , $\Gamma/\nu = 3000$.

and Kop'ev & Chernyshev (1993). (iii) The observations of Maxworthy (1977) of the development of swirling flow and a solitary bulge wave following the Widnall instability.

2. Methods

Calculations were performed using a second order finite difference code in cylindrical coordinates (x, r, ϕ) assuming axial periodicity (with length L_x) and a slip wall at $r = R_o$ as described in Verzicco & Orlandi (1993). The spurious straining due to the infinite row of rings and due to the wall is estimated to be less than 2% of the strain (due to ring curvature) which drives the instability. Units are chosen so that the circulation, Γ, and ring radius, R, are unity. To avoid effects of axisymmetric unsteadiness, a ring with an initially Gaussian core (of radius $\sigma = .4131$) and $\Gamma/\nu = 3000$ was axisymmetrically relaxed to a quasi steady state in which ω_ϕ/r becomes some function of the streamfunction. The number of grid intervals in each direction is 128 with a smaller radial spacing, obtained by a non uniform mesh, near the vortex core. The domain size is $R_o = L_x = 6$. A random divergence-free perturbation is applied to the basic-state velocity.

The acoustic pressure, p_a, is obtained from the theory of Möhring (1978):

$$p_a = \frac{\rho_o}{c_o^2}\frac{x_i x_j}{\Delta^3} Q_{ij}'''(t - \Delta/c_o), \quad Q_{ij} \equiv \frac{1}{12\pi}\int x_i(\mathbf{x}\times\boldsymbol{\omega})_j \, d^3x, \tag{1}$$

where $\Delta \equiv x_i x_i$. The triple prime denotes the third time derivative and is numerically evaluated using cubic splines. Due to the factor $x_i x_j$ only the symmetrized Q_{ij} are required, and in cylindrical coordinates one obtains:

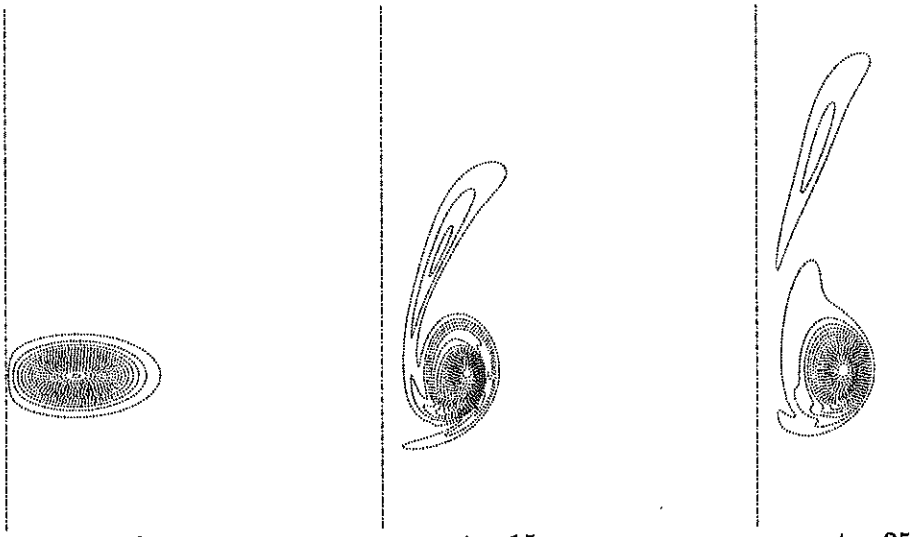

FIGURE 2. Contour-plots of azimuthal vorticity fon an elliptically distorted Gaussian core vortex ring at $\Gamma/\nu = 3000$. Contour increments are $\Delta = 0.1$, —·— , axis of symmetry. The ring motion is downward.

$$\begin{aligned}
Q_{11} &= 2\pi I_1 \text{ (0 mode only)} \\
Q_{22} &= \frac{\pi}{2}(K_1 - I_4 - 2I_1 - I_8) \text{ (0 and 2 modes)} \\
Q_{33} &= \frac{\pi}{2}(I_4 - 2I_1 + I_8 - K_1) \text{ (0 and 2 modes)} \\
Q_{12} + Q_{21} &= \pi(I_2 - J_1 - J_2 + K_3) \text{ (1 mode only)} \\
Q_{13} + Q_{31} &= \pi(J_4 - J_3 - I_3 + K_2) \text{ (1 mode only)} \\
Q_{23} + Q_{32} &= \pi(I_6 - I_7 - K_5) \text{ (2 mode only)}
\end{aligned} \tag{2}$$

The various integrals in Eq. (2) are

$$\begin{aligned}
&I_1 = \int xr^2\widetilde{\omega}_\phi(0)\,dxdr, \quad I_2 = \int xr^2\widehat{\omega}_x(1)\,dxdr, \quad I_3 = \int xr^2\widetilde{\omega}_x(1)\,dxdr, \\
&I_4 = \int xr^2\widehat{\omega}_r(2)\,dxdr, \quad I_6 = \int xr^2\widetilde{\omega}_r(2)\,dxdr, \quad I_7 = \int xr^2\widehat{\omega}_\phi(2)\,dxdr, \\
&I_8 = \int xr^2\widetilde{\omega}_\phi(2)\,dxdr, \quad J_1 = \int x^2r\widehat{\omega}_r(1)\,dxdr, \quad J_2 = \int x^2r\widetilde{\omega}_\phi(1)\,dxdr, \\
&J_3 = \int x^2r\widehat{\omega}_\phi(1)\,dxdr, \quad J_4 = \int x^2r\widetilde{\omega}_r(1)\,dxdr, \quad K_1 = \int r^3\widehat{\omega}_x(2)\,dxdr, \\
&K_2 = \int r^3\widehat{\omega}_\phi(1)\,dxdr, \quad K_3 = \int r^3\widetilde{\omega}_\phi(1)\,dxdr, \quad K_5 = \int r^3\widetilde{\omega}_x(2)\,dxdr,
\end{aligned} \tag{3}$$

where, for instance, $\widehat{\omega}_x(m)$ and $\widetilde{\omega}_x(m)$ denote the mth sin and cos azimuthal modes, respectively, of the axial vorticity. Note that only the modes $m \leq 2$ are involved.

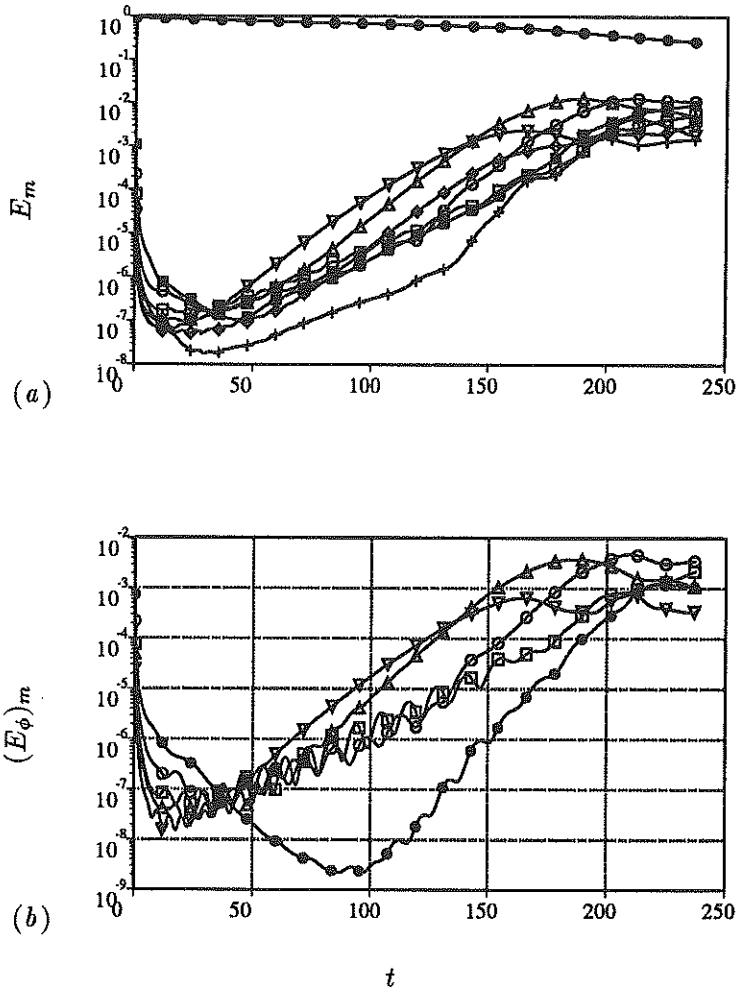

FIGURE 3. Evolution of energy in azimuthal modes. Mode index m: ● , 0; ■ , 1; ○ , 2; □ , 3; △ , 4; ◇ , 5; ▽ , 6; + , 7. (a) Total energy. (b) Energy in azimuthal velocity component. Certain modes have been omitted for clarity.

The theory of Möhring is valid for an unbounded domain in which the vorticity decays exponentially at infinity. This holds provided the computational domain is large compared with the vortical region. As the ring leaves and re-enters the period, what its position would be in an unbounded domain is tracked in order to obtain an x value in the unbounded domain for every grid point. The field is phase shifted axially so that the vortical region is centered in the integration domain and mid-point rule quadrature is employed. To assess errors due to out-lying vorticity, integration is also performed in a smaller domain of radial and axial dimensions $R_T = 5R_o/6$ and $L_T = 5L_x/6$, respectively. As a test, the acoustic signal for an axisymmetric ring with an elliptically distorted Gaussian core was obtained (Fig. 1).

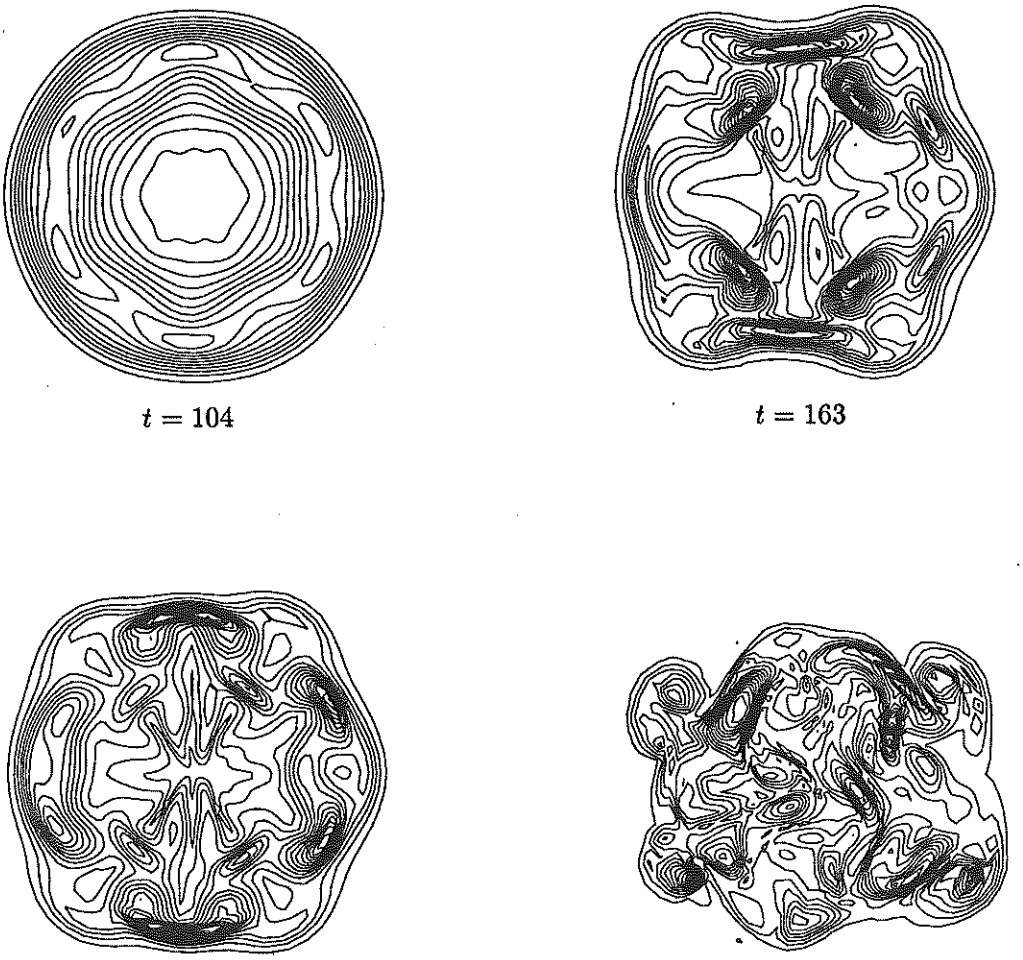

FIGURE 4. Contours of vorticity magnitude in the (r, θ) plane of maximum $\mid \omega \mid$. The spatial resolution of the simulation is twice the resolution of the figure.

It has the form of a damped cosine. The damping is due to the readjustment of the initial vorticity distribution towards an equilibrium distribution (Fig. 2). For an inviscid axisymmetric elliptic core ring with uniform vorticity, the acoustic signal is easily worked out (Shariff *et al.* 1989, p. 112) from the dynamics of Moore (1980). For the present case it is an undamped cosine with amplitude .022 which is close to the initial amplitude computed. Also, the period of the acoustic signal agrees with the theoretical prediction.

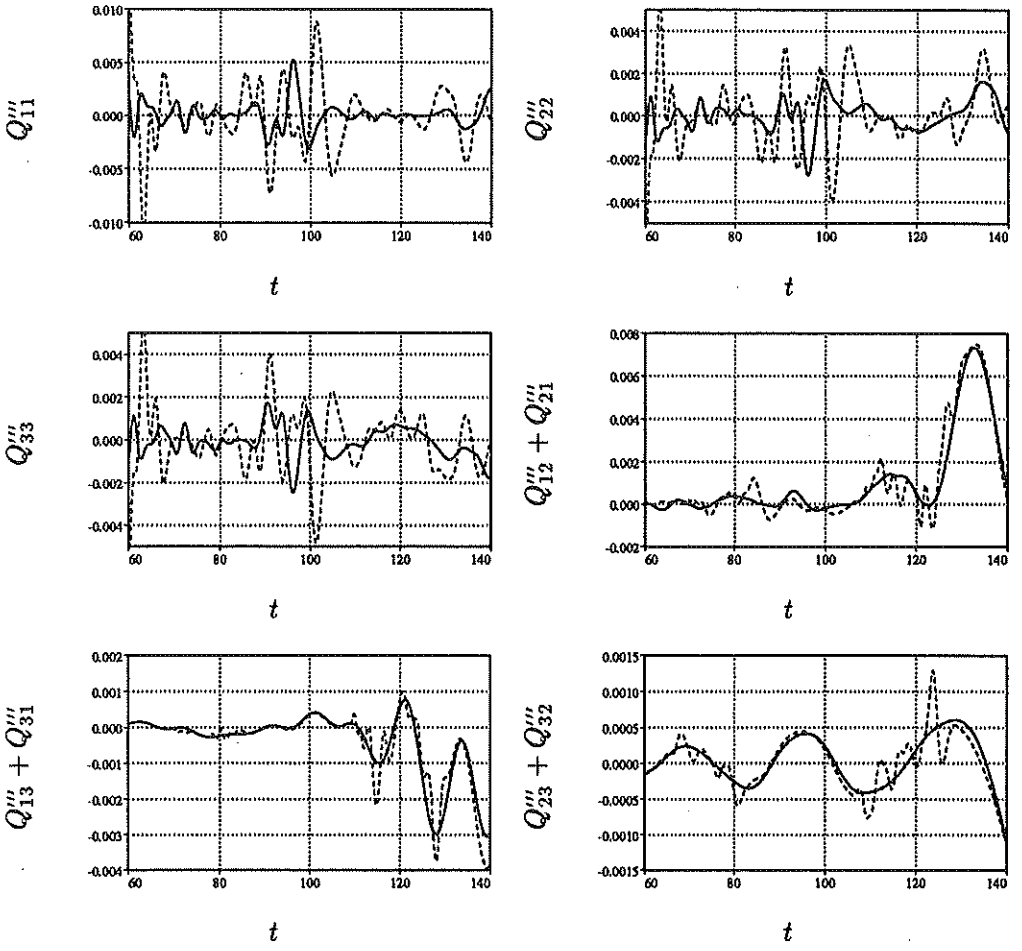

FIGURE 5. Acoustic components. ——— , Full-domain; - - - - , Truncated domain.

3. Results

Applying the inviscid stability theory of Widnall *et al.* (1974), valid for thin cores, to the Gaussian profile, one finds that the so-called 'non-rotating second radial mode' corresponds to $m = 2.26R/\sigma = 5.47$ so that either $m = 5$ or 6 should be most unstable. The theory also predicts that there should be a band of growing modes around the most unstable one. Fig. 3*a* shows that the numerical result is consistent with this picture. Since the initial perturbation is not a combination of eigenmodes, there is an initial transient, after which the $m = 6$ mode is dominant showing a large range of linear growth. At $t = 150$ the $m = 6$ mode gives way to $m = 4$, likely due to viscous spreading of $\sigma(t)$; this switching of the dominant mode has also been previously observed by Hasselbrink (1992) and Shariff *et al.* (1994). At later times the non-linearly amplified $m = 1$ and 2 modes become dominant and all modes saturate. That the overall ring shape follows the dominant mode is shown in Fig. 4 where contour plots of $|\omega|$ in the (r, ϕ) plane of maximum $|\omega|$ are

displayed.

Maxworthy (1977) used dye visualization to infer that following breaking of the instability wave, a swirling flow developed in the azimuthal direction accompanied by a propagating solitary bulge wave. Fig. 3*b* plots modal energies in the azimuthal velocity component to illustrate the rapid development of a mean swirl (•). This fact together with the nonlinear growth of the $m = 1$ wave already shown in Fig. 3*a* may be related to Maxworthy's observation.

Fig. 5 shows contributions to the acoustic signal during the linear instability phase comparing the results for the full and truncated integration domains. For the diagonal terms the two domains have differences comparable to the amplitude. These terms involve the $m = 0$ and $m = 2$ modes. The off-diagonal terms have smaller differences mainly in the form of high frequency oscillations present in the truncated domain. The particle turn-around time is about 12 initially, and it corresponds to the period of acoustic oscillations due to an elliptically distorted core. On the other hand, the term $Q'''_{23} + Q'''_{32}$, which involves only the $m = 2$ mode, has a larger period. This is consistent with the frequency ratio of the two modes for thin uniform vorticity cores: using Eq. (35) in Widnall & Sullivan (1973) we obtain

$$\frac{f_{\text{elliptic ring}}}{f_{\text{elliptic core}}} = \sqrt{3}\frac{a^2}{R^2}\log(a/R),$$

which gives an estimate of 0.3 for the present case (a is the radius of the uniform vorticity core).

Further work using the same method should either focus on the sound for axially periodic flow (cylindrical wavefronts at infinity) using the appropriate acoustic analogy or employ a larger domain.

4. Conclusions

The time evolution of azimuthal instabilities on a thick isolated vortex ring into the late non-linear stage was studied by a numerical simulation of the Navier-Stokes equations. Initially the $m = 6$ mode is most amplified, consistent with the linear theory of Widnall *et al.* (1974). Subsequently, due to the viscous spreading of the ring, the $m = 6$ gave way to $m = 4$. In the late non-linear stage low order modes ($m = 2$ and $m = 1$) became dominant and a rapid growth of a mean swirl is present, which may be related to some dye observations of Maxworthy (1977).

The acoustic signal computed using the theory of Möhring (1978) was presented for the linear instability phase. Since this theory is valid for unbounded flow, each contribution (Q_{ij}) was computed in a full and in a truncated domain to estimate errors associated with outlying vorticity. The errors were quite large for the diagonal terms. Further work is needed to eliminate these errors.

REFERENCES

BRIDGES, J. E. & HUSSAIN, A. K. M. F. 1987 Roles of initial condition and vortex pairing in jet noise. *J. Sound. Vib.* **117**, 289–311.

HASSELBRINK, E. F. 1992 Breakdown and mixing in a viscous circular vortex ring. BS thesis, Dept. of Mech. Eng., Univ. Houston.

KOP'EV, V. F. & CHERNYCHEV, S. A. 1993 Sound radiation by high frequency oscillations of the vortex ring. AIAA Paper 93-4362. 15th Aeroacoustics Conf.

MAXWORTHY, T. 1977 Some experimental studies of vortex rings. *J. Fluid Mech.* **81**, 465–95.

MÖHRING, W. 1978 On vortex sound at low Mach number. *J. Fluid Mech.* **85**, 685–691.

MOORE, D. W. 1980 The velocity of a vortex ring with a thin core of elliptical cross-section. *Proc. Roy. Soc. Lond. A.* **370**, 407–415.

SHARIFF, K. & LEONARD, A. 1992 Vortex rings. *Ann. Rev. Fluid Mech.* **24**, 235–279.

SHARIFF, K., LEONARD, A. & FERZIGER, J. H. 1989 Dynamics of a class of vortex rings. NASA TM 102257

SHARIFF, K., VERZICCO, R. & ORLANDI, P. 1994 A numerical study of three-dimensional vortex ring instabilities: viscous corrections and early non-linear stage. *J. Fluid Mech.* **279**, 351–375.

VERZICCO, R. & ORLANDI, P. 1993 A finite-difference scheme for three-dimensional incompressible flows in cylindrical coordinates. Submitted to *J. Comput. Phys.*

WIDNALL, S. E., BLISS, D. B. & TSAI, C.-Y. 1974 The instability of short waves on a vortex ring. *J. Fluid Mech.* **66**, 35–47.

WIDNALL, S. E. & SULLIVAN, J. P. 1973 On the stability of vortex rings. *Proc. Roy. Soc. Lond. A.* **332**, 335–353.

ZAITSEV, M. Y., KOP'EV, V. F., MUNIN, A. G. & POTOKIN, A. A. 1990 Sound radiation by a turbulent vortex ring. *Sov. Phys. Dokl.* **35**, 488-489.

ZAITSEV, M. Y. & KOP'EV, V. F. 1993 Mechanism of sound generation by a turbulent vortex ring. *Acoust. Phys.* **39**, 562–565.